# Chiral Siderophore Analogs: Ferrichrome

**Izac Dayan, Jacqueline Libman, Yael Agi, and Abraham Shanzer***

Department of Organic Chemistry, The Weizmann Institute of Science, Rehovot, Israel

*Received October 30, 1992*

Two novel families of chiral trishydroxamate binders are described. These compounds have been modeled after the natural siderophore ferrichrome in an attempt to mimic its biological properties as iron(III) carrier and growth promoter. In these analogs the hydroxamate binding sites and tripodal topology of ferrichrome are retained, but the chiral hexapeptide anchor of the natural siderophore is replaced by $C_3$-symmetric tricarboxylates of two homologous types ($m$ = 1, type 1; $m$ = 2, type 2). The resulting loss of chirality is compensated by symmetric extension of these anchors with natural amino acids (Figure 1). In this design two elements are of particular importance: (i) the amino acid bridges that induce chirality, stabilize specific conformations of the free ligands, and allow systematic modifications and (ii) the use of two homologous anchors that dictate the conformations of the metal complexes. Type 2 binders proved to either simulate the performance of the natural ferrichrome and act as growth promoters or to inhibit the action of ferrichrome and function as growth inhibitors. On the other hand, none of the type 1 binders proved active. In an attempt to establish the origin of these differences, the structures of the two types of compounds and of their octahedral metal complexes are examined by a combination of IR, NMR, UV/vis, CD, and NMR spectroscopy. Little differences were observed in the conformations of the free ligands as both types adopt propeller-like arrangements that are stabilized by intramolecular H-bonds. Both types of complexes also predominantly assume the Λ-cis configuration when L-amino acids are used. However, pronounced differences were observed in the conformations of the metal complexes: while in type 1 complexes the amides are positioned tangentially to the molecules cross section, in type 2 complexes they are oriented radially with the amide-NH pointing inward. In the latter arrangement the amide-NH groups become fit to form intramolecular H-bonds. These findings allowed us to interpret the in vivo performance of these compounds and to identify the structural requirements for obtaining growth promoters or growth inhibitors, respectively. The systematically modified ligands allowed us to examine the effect of intramolecular interactions, specifically H-bond networks and van der Waals forces, on the complexes' stoichiometry and isomeric and optical purity. The presence of either of the two intramolecular forces is sufficient to obtain monomeric complexes of 1:1 stoichiometry, while the absence of both like in the glycine derivative of type 1 ligand, **1G**, causes the formation of polymeric complexes.

## 1. Introduction

Recently we prepared chiral triscatecholates[1] that simulate enterobactin[2,3] in exhibiting high binding efficiency for iron(III) and adopting predominantly the right-handed configuration around the metal core. These binders were assembled from $C_3$-symmetric trisamines as anchors, symmetrically extending amino acid residues as bridges, and terminating catecholamides as binding sites.[1] The crucial elements in these binders are the bridging amino acids that introduce chirality to the ligands and generate networks of intramolecular H-bonds. These H-bonds fulfill a 2-fold task: In the free ligands they interlink the molecule's individual strands toward a propeller-like conformation that is prone to ion binding, and upon ion binding they rearrange to stabilize the complex formed.[1]

Here we apply this strategy of design and modular buildup to the preparation of another siderophore analog, namely ferrichrome.[4] Ferrichrome has been shown to act as microbial iron(III) carrier and growth promoter by traversing the cellular membrane through the intervention of highly specific membrane receptors and transport proteins.[5] Ferrichrome,[6] similarly to enterobactin, is built from a macrocyclic ring as anchor which bears three ion binding side chains that create an octahedral ion binding cavity. Ferrichrome however differs from enterobactin by lacking $C_3$ symmetry, possessing hydroxamate groups rather than catecholates as ion binding sites, and adopting the Λ-cis configuration when binding iron. In order to obtain ferrichrome analogs that would adopt the biologically active, naturally occurring Λ-cis configuration and form favorable H-bond networks, two alternative strategies can a priori be considered, attachment of *N*-hydroxy-amino acid residues of D-configuration to trisamines as anchors or attachment of amino acid residues of L-configuration to triscarboxylates. We optioned for the latter alternative, which can draw from natural amino acids as building blocks, and selected two homologous triscarboxylates as anchors, type 1 and type 2 ($m$ = 1, $m$ = 2, Figure 1), that differ in the length of their methylene chains. This design necessarily inverts the directionality of the terminal hydroxamate groups relative to that occurring in ferrichrome. This inversion was however thought not to curtail biological activity, since retroferrichrome has been shown to equal ferrichrome as a microbial iron(III) carrier and growth promoter.[7]

(1) Tor, Y.; Libman, J.; Shanzer, A.; Lifson, S. *J. Am. Chem. Soc.* **1987**, *109*, 6517. Tor, Y.; Libman, J.; Shanzer, A.; Felder, C. E.; Lifson, S. *J. Am. Chem. Soc.* **1992**, *114*, 6661.

(2) Raymond, K. N.; Carrano, C. J. *Acc. Chem. Res.* **1979**, *12*, 183. Raymond, K. N.; Mueller, G.; Matzanke, B. F. *Top. Cur. Chem.* **1984**, *123*, 49. Hider, R. C. *Struct. Bonding* **1984**, *58*, 25. Shanzer, A.; Libman, J.; Lifson, S.; Felder, C. E. *J. Am. Chem. Soc.* **1986**, *108*, 7609.

(3) Harris, W. R.; Raymond, K. N. *J. Am. Chem. Soc.* **1979**, *101*, 6534. Pecoraro, V. L.; Weitl, F. L.; Raymond, K. N. *J. Am. Chem. Soc.* **1981**, *103*, 5133. Harris, W. R.; Raymond, K. N.; Weitl, F. L. *J. Am. Chem. Soc.* **1981**, *103*, 2667.

(4) For a preliminary communication on this work see: Tor, Y.; Libman, J.; Shanzer, A. *J. Am. Chem. Soc.* **1987**, *109*, 6518.

(5) Burnham, B. F.; Neilands, J. B. *J. Biol. Chem.* **1960**, *236*, 554. Emery, T. *Biochemistry* **1971**, *10*, 1483. Van der Helm, D.; Baker, J. R.; Eng-Wilmot, D. L.; Hossain, M. B.; Loghry, R. A. *J. Am. Chem. Soc.* **1980**, *102*, 4224.

(6) *Iron Transport in Microbes, Plants and Animals*; Winkelmann, G., van der Helm, D., Neilands, J. B., Eds.; VCH Verlagsgesellschaft mbH: D-6940 Weinheim, Germany, 1987. Winkelmann, G.; Braun, V. *FEMS Microbiol. Lett.* **1981**, *11*, 237.

(7) Emery, T.; Emery, L.; Olsen, R. K. *Biochem. Biophys. Res. Commun.* **1984**, *119*, 1191.

0020-1669/93/1332-1467$04.00/0 

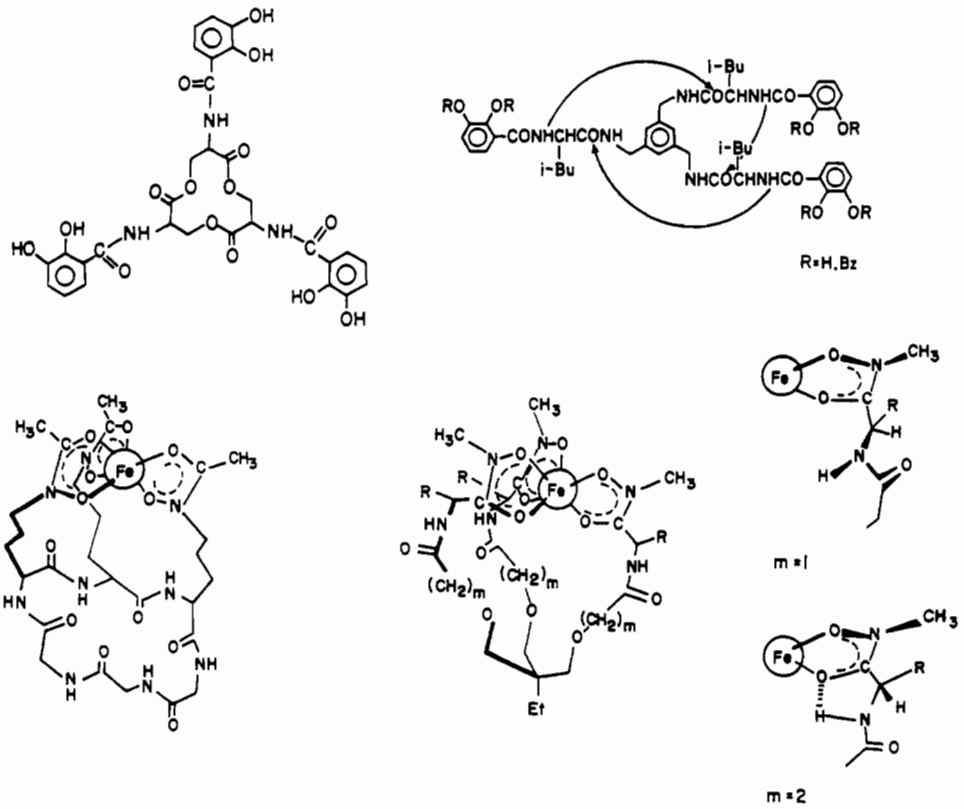


**Figure 1.** Enterobactin (top left), biomimetic enterobactin analogs (top right), ferrichrome (bottom left), and biomimetic ferrichrome analogs (bottom right).

Two elements are of particular importance in this design: (i) the use of amino acids as bridges that introduce chiral centers, stabilize specific conformations of the free ligands, and allow for systematic modifications and (ii) the use of two homologous tricarboxylates as anchors that dictate the conformations of the metal complexes. Homologous variations of methylene chains from even- to odd-numbered members are well-known to effect physicochemical characteristics of linear molecules and have been demonstrated to have a pronounced effect on the conformations of macrocyclic compounds.[8,9] Since octahedral metal complexes of tripodal molecules can be regarded as polycyclic structures, the effect of homologous variations was expected to be even further amplified and to result in conformationally different, but well-defined, arrangements.

Several families of trishydroxamate binders have earlier been described,[10] some found to exert remarkably high iron(III) binding efficiencies and some to act as growth promoters of specific microorganisms. The binders introduced here differ from the earlier ones by their chirality and modular assembly that allows systematic modifications of the complexes' spatial requirements and conformations till optimal fit to the microbial receptor is obtained. And indeed, representatives of type 2 binders were found to exert varying degree of biological activity. Some proved to simulate the performance of ferrichrome in vivo by being recognized by the respective membrane receptor and transport proteins, while others were shown to inhibit its action by competing for its membrane receptor.[11-13] On the other hand, none of the type 1 binders proved active.[12] These differences between type 2 and type 1 binders were thought to derive from conformational differences of their iron(III) complexes that are imposed by the homologous relationships of their anchors.

In this article we aim at establishing the origin of the different biological activity of these two types of binders in terms of their conformational parameters. Toward this end we examine the conformations of the free ligands and of their metal complexes by a combination of IR, NMR, UV/vis, and CD spectroscopy while putting emphasis on elucidating the similarities and differences of the two types of compounds.

## 2. Results and Discussion

**2.1. Synthesis.** The assembly of the ferrichrome analogs described here relies on tricarboxylates **3** and **4** as anchors, amino acids (ala, leu, gly, pro, and ileu) as bridges, and terminal hydroxamate groups as iron binding sites. In line with the compounds' modular design, their synthesis was accomplished by stepwise assembly of essentially three units: (i) the triscarboxylates as anchors, (ii) the amino acids as bridges, and (iii) the terminating hydroxamate groups as ion binding sites. The synthesis involved the following steps: (i) preparation of the triscarboxylate anchors **3** and **4**, respectively, from 1,1′,1″-tris-(hydroxymethyl)propane,[14] (ii) condensation of the selected amino acids with hydroxyl amine to the hydroxamate bearing amino acid bridges **5**, and (iii) coupling of the amino acid bridges with the triscarboxylate anchors to the final products of type 1 ($m$ = 1) and type 2 ($m$ = 2) (Figure 2). The parent hydroxamates **1** and **2** were prepared by direct coupling of the triscarboxylate anchors **3** and **4** with methylhydroxylamine as indicated below.

**2.2. Structure of Free Ligands.** The structures of the free

(8) Shanzer, A.; Libman, J.; Frolow, F. *Acc. Chem. Res.* **1983**, *16*, 60.
(9) Lifson, S.; Felder, C. E.; Shanzer, A.; Libman, J. *Progress in Macrocyclic Chemistry*; Izatt, R. M., Christensen, J. J., Eds.; John Wiley and Sons, Inc.: New York, 1987; Vol. 3, p 241.
(10) Lee, B. H.; Miller, M. J.; Prody, C. A.; Neilands, J. B. *J. Med. Chem.* **1985**, *28*, 317. Mitchell, M. S.; Walker, D. L.; Whelan, D. L.; Bosnich, B. *Inorg. Chem.* **1987**, *26*, 396. Akiyama, M.; Katoh, A.; Muto, T. *J. Org. Chem.* **1988**, *53*, 6089. Ng, Y. C.; Rodgers, S. J.; Raymond, K. N. *Inorg. Chem.* **1989**, *28*, 2062.
(11) Shanzer, A.; Libman, J.; Lazar, R.; Tor, Y.; Emery, T. *Biochem. Biophys. Res. Commun.* **1988**, *157*, 389.
(12) Jurkevitch, E.; Hadar, Y.; Chen, Y.; Libman, J.; Shanzer, A. *J. Bacteriol.* **1992**, *174*, 78.
(13) Shanzer, A.; Libman, J. *CRC-Handbook of Microbial Iron Chelates*; Winkelmann, G., Ed.; CRC Press, Inc.: Boca Raton, FL, 1991; p 309.
(14) Dayan, I.; Libman, J.; Shanzer, A.; Felder, C. E.; Lifson, S. *J. Am. Chem. Soc.* **1991**, *113*, 3431.

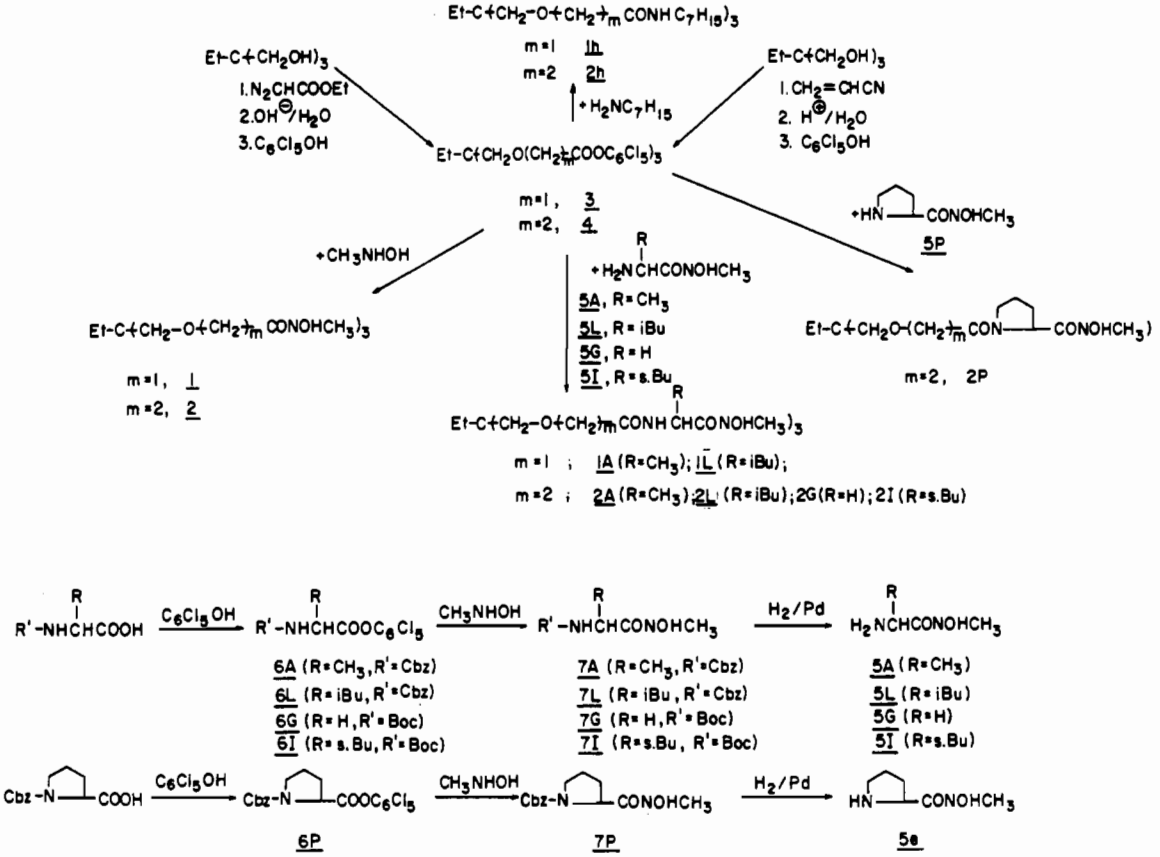



**Figure 2.** Synthetic schemes for the preparation of the hydroxamate binders. (A stands for alanyl-, L for leucyl-, G for glycyl-, I for ileucyl-, and P for prolyl-containing intermediates and final products.)

**Table I.** IR Data ($\nu$/cm$^{-1}$) for the Free Ligands

| | NH | | CONHR amide I | | CONHR amide II | | CON | |
|---|---|---|---|---|---|---|---|---|
| compd | *a* | *b* | *a* | *b* | *a* | *b* | *a* | *b* |
| **1**[c] | | | | | | | | 1638 (KBr) |
| **1A** (ala) | 3397, 3203 (br) | | 1642 | 1678 | 1528 | 1520 | 1642 | 1654 |
| **1L** (leu) | 3408, 3244 (br), 3155 | | 1642 | 1681 | 1531 | | 1642 | 1656 |
| **1G** (gly)[c] | | | | 1633 | | | | 1633 |
| **1h** | 3433 | 3410 | 1672 | 1674 | | | | |
| **2** (20 mM) | 3259 | 3320 | | | | | 1638 | 1649 |
| **2A** (ala) | 3280 | | 1632 | | 1531 | | 1632 | |
| **2L** (leu) | 3284 | 3315 | 1630 | 1651 | 1529 | 1535 | 1630 | 1635 |
| **2G** (gly)[c] | | | | 1641 | | | | 1641 |
| **2I** (ileu) | 3300 | | 1629 | | | | 1629 | |
| **2P** (pro) | 3189 | | 1615 | 1637 | 1453 | 1453 | 1638 | 1637 |
| **2h** | 3451, 3382 | | 1657 | 1669 | | | | |

[a] In 10 mM $CDCl_3$ unless otherwise stated. [b] In 10 mM $CD_3CN$ unless otherwise stated. [c] The compound is insoluble in $CDCl_3$.

ligands, and particularly the occurrence of intramolecular H-bonds, was tested by examining their IR and NMR spectra in apolar and polar solvents and by comparing these data with those of selected reference compounds. As reference compounds we used two kinds of structures: the tripodal trishydroxamates **1** and **2** that lack the intermittent amino acid bridges and the tripodal trisamides **1h** and **2h** that lack the terminating hydroxamate binding sites.[14]

The IR spectra of the parent amide **1h** show high-frequency carbonyl and NH absorptions in chloroform and moderate solvent effects when replacing chloroform by acetonitrile, implying the lack of H-bonds (Table I). On the other hand, the hydroxamate ligands of type I possessing ala or leu bridges **1A** or **1L** exhibit low-frequency amide and hydroxamate carbonyl absorptions and mostly low-frequency NH absorptions in chloroform solution, suggesting the presence of intramolecular H-bonds. When apolar chloroform is replaced by polar acetonitrile, a substantial blue shift occurs to values that are close to those of the parent amide **1h** carbonyl, indicating cleavage of the H-bonding network.

The trishydroxamates of type 2 exhibit similar, but not identical, patterns. The chiral trishydroxamates **2** with ala, leu, and ileu bridges have consistently low-frequency carbonyl and NH absorptions in chloroform, indicating the presence of an extensive H-bonding network, and exert blue shifts of their carbonyl and amide NH absorptions when replacing chloroform by acetonitrile, indicating partial cleavage of the H-bonds. The parent trisamide **2h**, in contrast to the parent trisamide **1h**, shows solvent-dependent carbonyl frequencies and some low-frequency NH absorption in chloroform, which indicates some H-bonding. Since amides of the same kind are unlikely to form interstrand H-bonds,[15] it is

(15) Tor, Y.; Libman, J.; Shanzer, A.; Felder, C. E.; Lifson, S. *J. Chem. Soc., Chem. Commun.* **1987**, 749. Tor, Y. Ph.D. Thesis, The Weizmann Institute of Science, Israel, 1990.

**Table II.** NMR Data ($\delta$/ppm) for the Free Ligands

| | chemical shift[a] | | | | | |
|---|---|---|---|---|---|---|
| | $CCH_2O$– | | | –$CH_2CO$– | | |
| compd | *b* | *c* | *d* | *b* | *c* | *d* |
| **1** | | | 3.46 (s) | | | 4.28 (s) |
| **1A** (ala) | 3.50, ABq (0.06) | 3.57 (s) | | 3.98, ABq (0.09) | 3.91 (s) | |
| **1L** (leu) | 3.48, ABq (0.07) | 3.49 (s) | | 3.98, ABq (0.09) | 3.94 (s) | |
| **1G** (gly) | | | 3.63 (s) | | | 4.19 (s) |
| **1h** | 3.45 (s) | 3.43 (s) | | 3.96 (s) | 3.84 (s) | |
| **2** | 3.41 (m) | 3.16 (s) | 3.20 (s) | 2.76 (m) | 2.65 (m) | 2.82 (t) |
| **2A** (ala) | 3.17, ABq (0.12) | 3.16 (s) | | 2.52 (m), 2.33 (m) | 2.38 (m) | |
| **2L** (leu) | 3.15, ABq (0.08) | 3.16 (s) | 3.19 (s) | 2.57 (m), 2.34 (2t) | | 2.47 (m) |
| **2G** (gly) | | | 3.31 (s) | | | 2.50 (t) |
| **2I** (ileu) | 3.12, ABq (0.08) | | | 2.55 (m), 2.35 (m) | | |
| **2P** (pro) | 3.22 (s) | 3.19, ABq (0.014) | 3.24 (s) | 2.60 (m), 2.52 (m) | 2.48 (m), 2.27 (m) | 2.73 (m), 2.51 (m) |
| **2h** | 3.25 (s) | 3.20 (s) | | 2.46 (m) | 2.28 (t) | |

[a] s stands for singlet, t for triplet, m for multiplet, ABq for AB quartet, and br for a broad signal. The values in parentheses are $\Delta\delta$ values for the ABq. [b] In 10 mM $CDCl_3$. [c] In 10 mM $CD_3CN$. [d] In 10 mM $CD_3OD$.

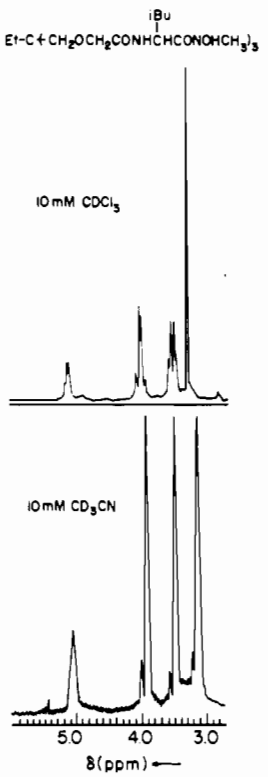


**Figure 3.** $^1$H-NMR traces of free ligand **1L** in $CDCl_3$ (top) and in $CD_3CN$ (bottom).

inferred that H-bonding in the trisamide **2h** takes place from the amide-NH to the ether oxygen.

NMR allowed us to establish the conformational consequences of the H-bonding networks in the chiral hydroxamates of types 1 and 2. The NMR spectra (Table II) of the chiral hydroxamate ligands of both types possessing ala, leu, or ileu bridges show nonequivalence of the diastereotopic –C–($CH_2O$–) protons in chloroform, indicating restricted conformational freedom. The extent of anisotropy remains constant over a 100-fold concentration range (between 0.1 and 10 mM), indicating that it derives from intramolecular interactions. This anisotropy collapses in the more polar solvent acetonitrile (Figure 3 and Table II).

The parallel solvent dependence of the IR and NMR spectra indicates that H-bonding and restricted conformational freedom (as expressed by the nonequivalence of the diastereotopic protons) are interrelated phenomena and thereby imply the presence of interstrand H-bonds in the chiral trishydroxamates of type 1 and type 2.

(16) The occurrence of the alternative intrastrand H-bonds forming five-membered rings has been demonstrated to be less likely; see ref 15.

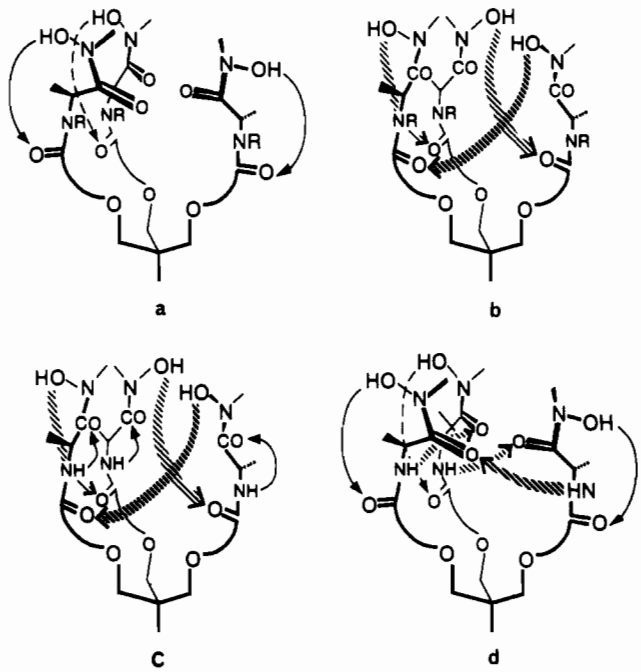


**Figure 4.** Schematic representation of possible H-bonding networks in free ligands: (a) Intrastrand H-bonds; (b) interstrand H-bonds; (c) and (d) combinations of both, intra- and interstrand H-bonds.[16]

Intramolecular H-bonds may be formed in two ways: (i) interstrand H-bonds between the amide carbonyl and hydroxamate NOH together with intrastrand H-bonds between the amide NH and hydroxamate carbonyl (Figure 4c) or (ii) interstrand H-bonds between the amide NH and hydroxamate carbonyls together with intrastrand H-bonds between the amide carbonyl and hydroxamate NOH (Figure 4d). Examination of the proline derivative **2P**, which lacks amide NH protons, allowed us to differentiate between the two alternatives. The amide carbonyls of **2P** show low-frequency absorptions in chloroform (Table I), indicating the occurrence of either intrastrand H-bonds (Figure 4a) or interstrand H-bonds (Figure 4b). The NMR equivalence of the diastereotopic protons –C–($CH_2O$) in chloroform excludes interstrand H-bonds and suggests structure 4a for trishydroxamate **2P**. The lack of interstrand H-bonds in **2P** demonstrates the necessity of the amide NH for interstrand H-bonds to occur and is in line with the conformation shown in Figure 4d for the chiral hydroxamates.

In summary, both types of chiral hydroxamates, types 1 and 2, when possessing ala, leu, or ileu bridges, are characterized by a fully H-bonded network in chloroform solution which involves both interstrand and intrastrand H-bonds.[17]

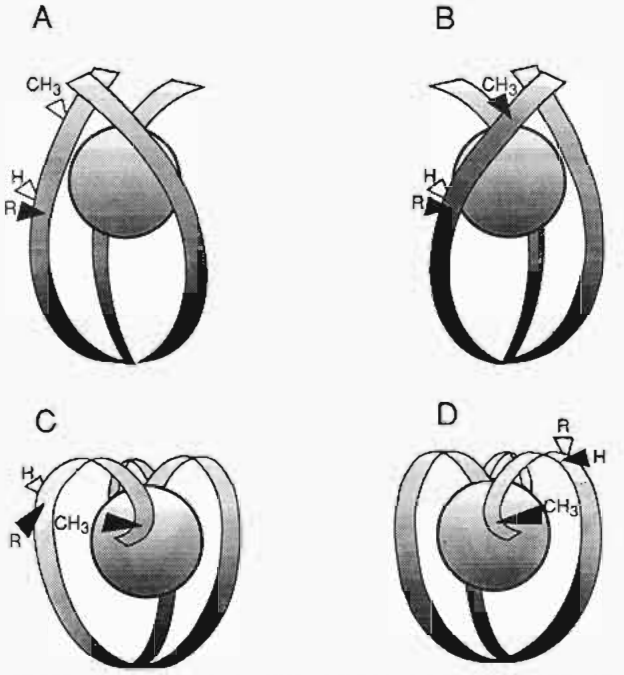


**Figure 5.** Schematic representation of alternative $C_3$-symmetric complexes. Group 1: (A) left handed; (B) right handed. Group 2: (C) left handed; (D) right handed.

**2.3. Ion Binding Properties.** Model building of possible tripodal $M^{3+}$ complexes reveals two groups of $C_3$-symmetric structures. In the first group, the hydroxamate binding sites are extended parallel to the molecules main axis in either a left- or right-handed twist. In the second group the hydroxamate binding sites are folded back relative to the molecules main axis forming either a left- or right-handed propeller. In the presence of chiral centers derived from L-amino acids the left-handed configuration appears stereochemically preferred in the first group (Figure 5A), but the right-handed appears preferred in the second one (Figure 5D).

As elaborated below, spectroscopic examination of the complexes allowed us to differentiate between these alternatives. The diamagnetic $Ga^{3+}$ complexes were examined by NMR,[18] which enabled us to determine the number of isomers formed and their symmetry. The paramagnetic $Fe^{3+}$ complexes were analyzed by UV and CD spectroscopy,[19] which allowed us to establish their preferred chiral sense. In addition both the $Fe^{3+}$ and $Ga^{3+}$ complexes were tested by IR,[20] in order to trace their H-bond networks.

When binding $Ga^{3+}$, the ligands may embed the metal in their internal cavity to form octahedral complexes of 1:1 stoichiometry or may generate multinuclear complexes. In cases of fast intermolecular and/or intramolecular equilibration, nonresolved $^1$H-NMR signals should be obtained for the diastereotopic protons. On the other hand, in cases of slow inter- and/or intramolecular equilibration, separate signals should be observed for the diastereotopic protons, thus enabling to establish the number and symmetry of the isomers formed.

The parent hydroxamate and gly derivative of type 2 show single sets of unresolved, somehow broadened peaks, suggesting the presence of fast interconverting mixtures of isomeric complexes of 1:1 stoichiometry.[21] Since intermolecular equilibration is slow in the NMR scale (free ligand and ligand–Ga complex give rise to separate sets of signals), the fast interconverting mixtures are attributed to derive from intramolecular equilibration. A single set of well-resolved signals was observed with type 1 leu and ala derivatives **1A** and **1L**, and type 2 leu derivative **2L** (Table III and Figure 6), demonstrating the presence of single isomers of $C_3$ symmetry. Two sets of well-resolved signals in a 2:1 ratio were obtained with the ala derivative of type 2, and more than two sets of signals for the pro derivative of type 2, indicating mixtures of isomers. The parent hydroxamate of type 1 formed an insoluble precipitate when treated with $Ga^{3+}$ but a clear solution when treated with $Al^{3+}$. The latter gave rise to a single set of signals with a fairly well resolved ABq for its $OCH_2CO$ protons, suggesting the presence of a single, $C_3$-symmetric chiral complex and of its enantiomer. The gly derivative of type 1 led to a complex, unresolved pattern when treated with $Ga^{3+}$, suggesting mixtures of complexes.

UV/vis titration of the trishydroxamate ligands with $FeCl_3$ in aqueous MeOH established 1:1 ion binding stoichiometry for most ligands, except for **1** and **1G**. CD spectroscopy of the 1:1 complexes established their preferred chiral sense. As evident from Table III, the ala, leu, and ileu derivatives of both types, types 1 and 2, show two Cotton effects, a positive one at longer wavelength (around 450 nm) and a negative one at shorter wavelength (around 360 nm),[5,19] demonstrating preferential (or possibly exclusive) Λ-cis configuration. The Cotton effects of the pro derivative **2P** were significantly smaller, indicating diminished chiral preference.

The properties of the $Fe^{3+}$ complexes are thus consistent with those of the corresponding $Ga^{3+}$ complexes. The chiral ligands that form isomerically pure $Ga^{3+}$ complexes show high dichroic values for their $Fe^{3+}$ complexes. The parent hydroxamate of type 2, as well as its gly derivative **2G**, provide well-defined $Ga^{3+}$ and soluble $Fe^{3+}$ complexes with normal extinction coefficients (Table III). The parent hydroxamate of type 1 yields insoluble $Ga^{3+}$ or $Fe^{3+}$ complexes, indicating the formation of multinuclear, polymeric species, and its gly derivative **1G** forms mixtures of $Ga^{3+}$ complexes and polymeric $Fe^{3+}$ complexes, as indicated by their low $R_f$ values on silica gel coated TLC plates.

These data taken together allow us to deduce the structures of the chiral complexes. The well-resolved NMR spectra of the chiral $Ga^{3+}$ complexes **1A**, **1L**, and **2L** are attributed to complexes of structure **1a** (Figure 5A), as their $Fe^{3+}$ analogs adopt the left-handed, Λ-cis configuration. The presence of two sets of well-resolved signals for the **2L**–Ga complexes excludes the presence of configurational isomers that can interconvert via intramolecular equilibration. Therefore the possibility of a nonsymmetric complex for **2L**–Ga, as well as the possibility of configurational isomers belonging to the same group of complexes (group 1 or group 2 in Figure 5) is excluded. We therefore attribute the two sets of signals to two isomers that equilibrate through intermolecular exchange processes, such as possibly occurring between the predominant left-handed structure **5a**, and the minor right-handed structure **5d**.

The similarity of both leu derivatives, **1L** and **2L**, in forming $Fe^{3+}$ and $Ga^{3+}$ of high isomeric purity, but the difference of the gly derivatives, **1G** and **2G**, where type 2 forms defined 1:1 complexes with $Fe^{3+}$ or $Ga^{3+}$, while type 1 fails to do so, is believed

(17) This behavior is in contrast to that observed in mesitylene- or amine-based $C_3$-symmetric trispeptides, where interstrand H-bonds are formed without the necessity of concurrent intrastrand H-bonds.[15] There are however differences between type 1 and type 2 hydroxamates. While in type 1 hydroxamates no H-bonds are retained in polar solvents, in type 2 hydroxamates some intrastrand H-bonds are still preserved. These intrastrand H-bonds are likely to occur between the ether oxygen and the amide NH groups to generate six-membered rings.

(18) Borgias, B. A.; Barclay, S. J.; Raymond, K. N. *J. Coord. Chem.* **1986**, *15*, 109.

(19) Cooney, R. P.; Reid, E. S.; Hendra, P. J.; Fleischmann, M. *J. Am. Chem. Soc.* **1977**, *99*, 2003.

(20) For earlier IR data on metal hydroxamates see: Chatterjee, B. *Coord. Chem. Rev.* **1978**, *26*, 293.

(21) The NMR spectra of 2Ga at lower temperatures revealed broadening of the $CH_2CO$ protons at –4 °C, and the spectra of **2G**–Ga broadening of the $NCH_2CO$ protons at –40 °C [the $C(CH_2O–)$ protons could not be seen because of overlap with $H_2O$], confirming that the lack of resolved signals is due to fast configurational interconversion and specifically to fast intramolecular interconversion. Intermolecular exchange appears slow on the NMR scale, as excess free ligand can readily be discerned by the appearance of separate sets of signals.

**Table III.** NMR, UV, and CD Spectral Data for the Metal Hydroxamates

| compd | $^1$H-NMR[a] C($CH_2O$), ppm (multiplicity) | compd | UV[b] $\lambda_{max}$, ($\epsilon$) | CD[b] $\lambda_{ex}$, nm ($\Delta\epsilon$) |
|---|---|---|---|---|
| **1**–Ga | ppt | **1**–Fe | 428 (1210) | |
| **1**–Al | 3.48 (ABq) | | | |
| **1A**–Ga | 3.68[c] (ABq, 0.30) | **1A**–Fe | 425 (2300) | 374, 420, 452 (–6.0, 0.0, +2.7) |
| **1L**–Ga | 3.65 (ABq, 0.20) | **1L**–Fe | 425 (2890) | 372, 420, 452 (–6.7, 0.0, +3.0) |
| **1G**–Ga | 3.5[d] (br, m) | **1G**–Fe | 430 (1600) | |
| **2**–Ga[20] | 3.36[e] (s) | **2**–Fe | 430 (2530) | |
| **2A**–Ga | 3.70; 3.48[f] (ABq, 0.49; ABq, 0.19) | **2A**–Fe | 426 (2210) | 365, 420, 455 (–7.5, 0.0, +2.5) |
| **2L**–Ga | 3.81[g] (ABq, 0.50) | **2L**–Fe | 424 (2500) | 365, 415, 450 (–6.8, 0.0, +3.43) |
| **2G**–Ga[20] | 3.65[d] (s) | **2G**–Fe | 434 (2870) | |
| | | **2I**–Fe | 418 (2730) | 368, 408, 444 (–7.4, 0.0, +4.4) |
| **2P**–Ga | mult signals | **2P**–Fe | 428 (2550) | 378, 430, 465 (–4.3, 0.0, +1.27) |

[a] The complexes were prepared in situ by treatment of the ligands in $CD_3CN$ (10 mM concentrations) with excess pyridine and subsequently $GaCl_3$ unless otherwise stated; s stands for singlet, t for triplet, m for multiplet, br for broad, and ABq for AB quartet. The values in parentheses are $\Delta\delta$ values for the ABq. [b] The spectra were recorded at 0.15–0.3 mM concentrations in aqueous MeOH (MeOH/0.1 N aqueous NaOAc = 1:1). [c] The compound examined contained at the tetrahedral carbon $CH_2$=$CHCH_2OCH_2$– instead of $C_2H_5$–. [d] The spectra were recorded in $CD_3OD$, 10 mM concentration. [e] The spectra were measured at 60 °C, to avoid overlap with $H_2O$ signals. [f] The ratio of the two signals corresponding to two isomers was found to be 2:1. [g] The values given are for the isolated complex in $CDCl_3$ solution. The values for the in situ prepared complex in $CD_3CN$ are only partial, because of overlap with $H_2O$ signals.

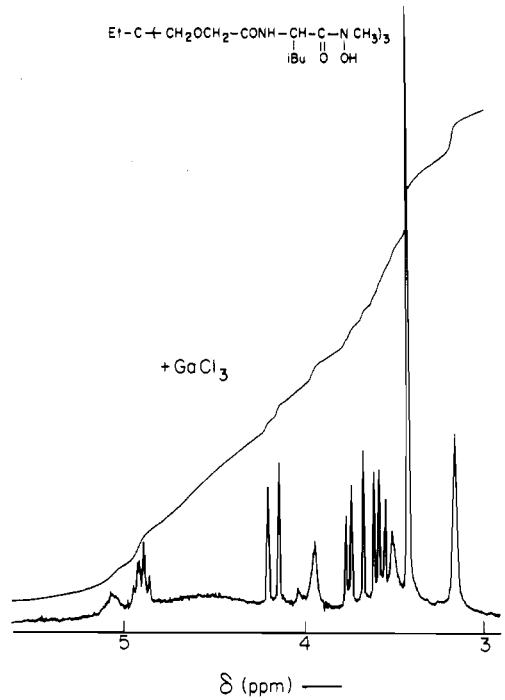


**Figure 6.** $^1$H-NMR trace of ligand **1L** in $CD_3CN$ after addition of $Ga^{3+}$.

to be significant. It is plausible to suggest that van der Waals interactions stabilize the 1:1 complexes of both leu derivatives, **1L** and **2L**, while the lack of this possibility in the gly derivative disfavors such complexes in **1G**, but not in **2G**. This in turn would suggest that other noncovalent interactions, i.e. H-bonding, might stabilize complexes derived from **2G**.

In order to examine this possibility, the IR spectra of representative $Fe^{3+}$ and $Ga^{3+}$ complexes of type 1 and type 2 were recorded in chloroform,[22] namely the complexes of the leu derivatives **1L** and **2L** and of the pro derivative **2P** (Tables I and IV).[20] As evident from Table IV, two major changes occur in the IR spectra of these ligands upon metal binding:[20] (i) a red shift of the hydroxamate carbonyl by 30–40 $cm^{-1}$ and (ii) a blue shift of the amide carbonyl by 20–35 $cm^{-1}$. The observed red shift of the hydroxamate carbonyl is similar to that observed for the parent hydroxamate **2** and is assigned to the metal hydroxamate chromophore.[20] The blue shifts of the amide C=O groups in the complexes of **1L** (+33 $cm^{-1}$), **2L** (+34 $cm^{-1}$), and to a minor extent in the complex of **2P** (+20 $cm^{-1}$), suggest conversion of the H-bonded amide C=O groups to nonbonded amide C=O groups.

This observation is compatible with cleavage of the intrastrand H-bonds between the hydroxamate NOH and amide C=O upon complexation for all cases. There is however a pronounced difference between the Fe complexes of **1L** and **2L**: while upon complexation of **1L** the NH absorption undergoes a significant blue shift to 3410 $cm^{-1}$, indicating free NH, the NH absorption of **2L** undergoes a smaller blue shift to 3350 $cm^{-1}$, indicating preservation of bonded NH (Figure 7). Since the carbonyl amides of **2L**–Fe are free, there are two alternative sites to which the amide NH can be bonded: either (i) the ether-oxygen as suggested in the trisamide **2h**, (ii) the metal(III)-bound carbonyl oxygen, C–O–Fe, or (iii) both. The second possibility is analogous to that occurring in the siderophore enterobactin and its synthetic analogs.[1,2]

The different H-bonding pattern of type 1 and type 2 complexes might explain the different ion binding properties of the gly derivatives **1G** and **2G**. It strongly suggests that stabilization of the complex by H-bonding in **2G** is essential for its formation in preference to polynuclear networks.

The role of H-bonds in type 2 complexes is further supported by comparing the isomeric purity of **2L**–Fe with that of **2P**–Fe, which lacks the possibility of H-bond stabilization. While **2L**–Fe showed a dichroic value of +3.43 at 450 nm, and **2L**–Ga a single set of signals in the $^1$H-NMR, the dichroic value for **2P**–Fe was lower by 60% and the $^1$H-NMR spectrum of **2P**–Ga showed more than a single set of signals (Table III).[23,24]

(22) The leu derivatives **1L** and **2L** were selected for IR studies because of their optical purity and high solubility in chloroform.

(23) The necessity of H-bond stabilization for high configurational purity in type 2, but not in type 1, may derive from the larger degree of freedom in the former (two methylene bridge between ether oxygen and amide carbonyl). Intramolecular H-bonds can constrain the molecule's conformation and the orientation of the side chains, thereby amplifying the energetic differences between the diastereoisomers.

(24) Information on the extent to which the H-bonding pattern affects binding strength was obtained by measuring the Mössbauer spectra of the solid complexes **2L**–Fe versus **2P**–Fe and by examining the temperature effect on their Mössbauer spectra as an indicator for the Fe–O bond strength.[25] From the area under the Mössbauer spectra as function of temperature ($T$), one obtains the temperature dependence of $\langle x^2 \rangle$ of the iron atoms. In the harmonic approximation, $\langle x^2 \rangle$ should be a linear function of $T$ and the slope should be proportional to the force constant, $A$. A comparison of the slopes obtained for **2L**–Fe and **2P**–Fe in the temperature range between 90 and 225 K shows that $A$(**2P**–Fe)/$A$(**2L**–Fe) = 1.09 ± 0.01. Though at higher temperatures the $\langle x^2 \rangle$ vs $T$ curve deviates from linearity, probably due to anharmonic effects, this estimate gives a crude indication of the ratios of the force constants involved and supports a larger force constant for **2L**–Fe than for **2P**–Fe.[26]

(25) Bauminger, R. Personal communication.

(26) Kolk, B. In *Dynamical properties of solids*; Horton, G. K., Maradudin, A. A., Eds.; North Holland: Amsterdam, 1984; Vol. 5, pp 63–90.

**Table IV.** IR Data ($\nu$/cm$^{-1}$) for the Metal Hydroxamates

| | NH | | CONHR amide I | | CONHR amide II | | CON | |
|---|---|---|---|---|---|---|---|---|
| compd | *a* | *b* | *a* | *b* | *a* | *b* | *a* | *b* |
| **1L**–Fe | 3410 | | 1675 | | 1526 | | 1600 | |
| **1L**–Ga | | | | 1684 | | 1521 | | 1611 |
| **2**–Fe (20 mM) | | | | | | | 1596 | |
| **2**–Ga | | | | | | | 1612 | |
| **2L**–Fe (15 mM) | 3346 | | 1664 | | 1524 | | 1601 | |
| **2L**–Ga | 3350 | | 1667 | | 1524 | | 1626, 1613 | |
| **2L**–Ga | | | | 1673 | | 1523 | | 1623, 1611 |
| **2P**–Fe (15 mM) | | | 1635 | | 1450 | | 1600 | |
| **2P**–Ga (6 mM) | | | 1631 | | 1452 | | 1604 | |

[a] Isolated complexes in 10 mM $CDCl_3$ unless otherwise stated. [b] The complexes were prepared in situ by treatment of the ligands in $CD_3CN$ (10 mM concentrations) with excess base and subsequently $GaCl_3$.

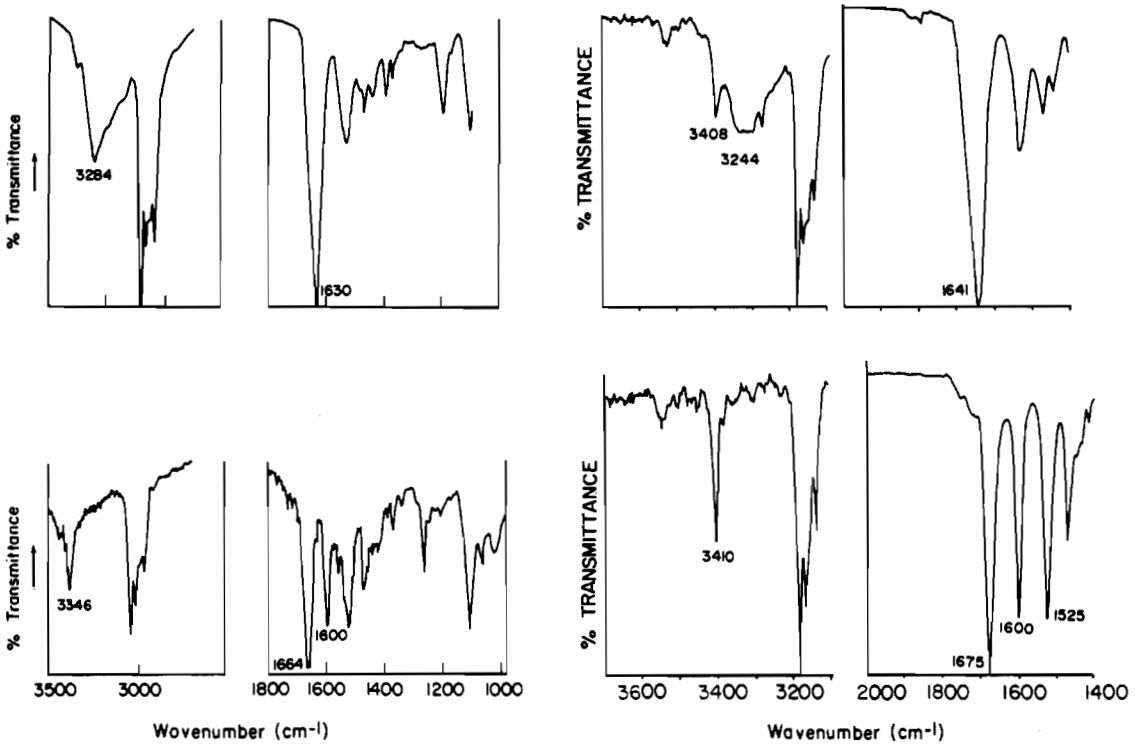


**Figure 7.** IR traces of ligands **1L** (top right) and **2L** (top left) and of their $Fe^{3+}$ complexes **1L**–Fe (bottom right) and **2L**–Fe (bottom left) all recorded in $CDCl_3$.

## 3. Summary and Conclusions

Examination of the two families of trishydroxamates allowed us to establish the effect of noncovalent interactions on the ligands' ion binding processes. Mutually supporting inter- and intrastrand H-bonds were found to shape the conformations of both types of ligands toward propeller-like arrangements in the free state. Upon binding, however, the behavior of the two types of ligands differed significantly. In type 2 derivatives the H-bonds were found to rearrange upon binding such as to stabilize the complexes formed. The latter type of rearrangement, which is reminiscent of the movement of a "windshield wiper", has earlier been suggested to occur in enterobactin[2] and its analogs[1] but escaped experimental verification because of the low solubility of catecholates in apolar solvents. In type 1 ligands, on the other hand, the H-bonds collapsed upon binding. The lack of intramolecular H-bonds in type 1 complexes is attributed to the nature of their anchor, which constrains the polycyclic metal complex such as to prohibit inward orientation of the amide-NH groups. Small structural changes at sites remote to the ion binding groups may thus drastically effect the conformations of the complexes, while being of minor consequence in the free ligands.

The systematic structural variations of the ligands at hand also enabled us to parametrize the effect of H-bonds and van der Waals forces on their ion binding properties. Comparison between the ligands demonstrated the necessity of either intramolecular H-bonds or van der Waals forces in order to obtain mononuclear complexes of 1:1 stoichiometry in preference to polymeric, polynuclear complexes.

The above findings also enabled us to interpret the in vivo performance of these ferrichrome analogs and to deduce the structural requirements for recognition by the respective membrane proteins. The biological activity of some of the L-amino acid derivatives of type 2, but lack of activity of their enantiomeric D-amino acid derivatives, is well in line with the documented chiral discrimination of the ferrichrome receptor.[11,12] Furthermore, the variations in the biological performance of type 2 derivatives permitted us to distinguish for the first time between the structural requirements for recognition by the membrane receptors and transporters, respectively,[12] to map the spatial requirements of the ferrichrome receptor and to trace differences of these requirements in different microorganisms.[11-13] The failure of the corresponding type 1 complexes to be recognized by the microbial iron(III) uptake system is attributed to the presence of exposed amide NH-groups, which appear to prohibit receptor binding because of repulsive forces. These pronounced differences in the in vivo performance of the two types of

ferrichrome analogs highlight the subtle structural demands at some domains, and remarkable tolerance at others, which may even allow replacement of a hexapeptide ring, as occurring in natural ferrichrome, by a simple triscarboxylate anchor.

## 4. Experimental Section

**General Methods.** Melting points were determined on a Fisher-Johns apparatus and are uncorrected. IR spectra were recorded on a Perkin-Elmer 681 grating spectrometer, a Fourier-transform IR Nicolet Mx-1 spectrometer, or Fourier-transform IR Cignus 25 Matteson spectrometer. Proton NMR spectra were measured on a Varian FT-80a or Bruker WH-270 NMR spectrometer. All chemical shifts are reported in $\delta$ units downfield from TMS as an internal standard. UV–vis spectra were measured on a Hewlett Packard Model 8450A diode array spectrophotometer, and CD spectra on a JASCO J-500C spectropolarimeter. Column chromatography separations were performed on silica gel Merck 70–230 mesh ASTM or on neutral alumina, flash column chromatography separations on silica gel Merck 230–400 mesh ASTM. THF was dried by treating overnight with KOH and subsequent filtration through basic alumina. Chloroform, methylene chloride, and acetonitrile were dried by filtration through basic alumina.

The homogeneity of the compounds was examined by thin-layer chromatography (mostly silica-coated plates, Merck), using at least two different solvent systems and two to three visualization methods (i.e. fluorescence quenching, jodine, ninhydrine, $FeCl_3$, etc).

The tripodal anchors **3** and **4** were prepared according to our earlier procedures.[14]

**Preparation of Cbz-L-NHCH(*i*-Bu)COOC$_6$Cl$_5$ (6L).** A 10.6-g amount (0.04 mol) of Cbz-L-leucine and 11.6 g (0.044 mol) of pentachlorophenol are dissolved in 300 mL of dried acetonitrile. A 7.8-mL volume (0.050 mol) of diisopropylcarbodiimide is then added at 0 °C. The solution is stirred over night at room temperature. The acetonitrile is removed and the crude mixture is chromatographed on silica gel ($CHCl_3$ or $CH_2Cl_2$) to give the desired product in 93% yield. Mp: 124–127 °C. IR ($CDCl_3$): $\nu$ 1784 ($COOC_6Cl_5$), 1724 cm$^{-1}$ (OCONH). $^1$H-NMR (270 MHz, $CDCl_3$): $\delta$ 7.35 (m, 5H, ArH), 5.16 (ABq, 2H, $CH_2Ar$), 4.76 (m, 1H, CH-*i*-Bu), and 1.01 ppm (m, 6H, $(CH_3)_2$).

**Preparation of Cbz-L-NHCH(CH$_3$)COOC$_6$Cl$_5$ (6A).** Using the same procedure as for active ester **6L**, ester **6A** is prepared and purified by flash chromatography on silica gel ($CH_2Cl_2$) to give the desired product in 60% yield. Mp: 177–178 °C. IR ($CDCl_3$): $\nu$ 1786 ($COOC_6Cl_5$), 1724 cm$^{-1}$ (OCONH). $^1$H-NMR (80 MHz, $CDCl_3$): $\delta$ 7.35 (m, 5H, ArH), 7.04 (d, 1H, $J$ = 7.8 Hz, NH), 5.15 (s, 2H, $ArCH_2$), 4.89 (m, 1H, CHMe), and 1.66 ppm (d, 3H, $J$ = 7.3 Hz, $CH_3$).

**Preparation of Boc-NHCH$_2$COOC$_6$Cl$_5$ (6G).** Boc-gly (5.95 g, 0.034 mol) is dissolved in 100 mL of dry methylene chloride, and the solution is treated with 9.06 g (0.034 mol) of pentachlorophenol, 1.52 g of (dimethylamino)pyridine, and 7.3 mL (0.046 mol) of diisopropylcarbodiimide for 1 day. Filter chromatography ($CHCl_3$) and recrystallization from chloroform provides active ester **6G** in 40% yield. Mp: 114–116 °C. IR ($CDCl_3$): $\nu$ 1791 ($COOC_6Cl_5$), 1717 cm$^{-1}$ (OCONH). $^1$H-NMR (270 MHz, $CDCl_3$): $\delta$ 4.31 (d, 2H, $NHCH_2CO$) and 1.46 ppm (s, 9H, $C(CH_3)_3$).

**Preparation of Boc-L-NHCH(*s*-Bu)COOC$_6$Cl$_5$ (6I).** Using the same procedure as for **6L**, the active ester **6I** is obtained in 36% yield after chromatography on neutral alumina ($CHCl_3$). Mp: 125–126 °C. IR ($CDCl_3$): $\nu$ 1779 ($COOC_6Cl_5$), 1715 cm$^{-1}$ (OCONH). $^1$H-NMR ($CDCl_3$): $\delta$ 4.67 (m, 1H, NH), 4.59 (m, 1H, CH-*s*-Bu), and 1.39 ppm (s, 9H, $C(CH_3)_3$).

**Preparation of Cbz-L-NCH$_2$CH$_2$CH$_2$CHCOOC$_6$Cl$_5$ (6P).** A 9.64-g amount (0.038 mol) of Cbz-L-proline and 10.56 g (0.04 mol) of pentachlorophenol are dissolved in 200 mL of dry acetonitrile. A 7.8-mL volume (0.050 mol) of diisopropylcarbodiimide is then added at 0 °C. The solution is stirred for 2 days at room temperature. Acetonitrile is removed, and the crude mixture is chromatographed on silica gel ($CHCl_3$) and on then neutral alumina ($CHCl_3$) to afford the desired product in 81% yield. Mp: 82–88 °C. IR ($CDCl_3$): $\nu$ 1789 ($COOC_6Cl_5$), 1704 cm$^{-1}$ (OCON). $^1$H-NMR (80 MHz, $CDCl_3$): $\delta$ 7.33 (m, 5H, ArH), 5.14 (s, 2H, $ArCH_2$), 4.75 (m, 1H, CH–), 3.63 (m, 2H, $NCH_2$), 2.39 (m, 2H, $CH_2$), and 2.04 ppm (m, 2H, $CH_2$).

**Preparation of Cbz-L-NHCH(*i*-Bu)CONOHCH$_3$ (7L).** A solution containing a 7-g amount (0.013 mol) of active ester **6L** dissolved in 80 mL of dry $CH_2Cl_2$ is added to a suspension containing 1.36 g (0.016 mol) of *N*-methylhydroxylamine hydrochloride, 2.275 mL of $Et_3N$, and 67 mg of *N*-hydroxysuccinimide in 65.5 mL of dry $CH_2Cl_2$. The solution is stirred for 2 days at room temperature. The solvent is distilled off, and the crude mixture is chromatographed on silica gel ($CHCl_3$ and then $CHCl_3$–MeOH, 99:1) to give the expected product in 62% yield. Mp: 71–73 °C. IR ($CDCl_3$): $\nu$ 1707 (OCONH), 1642 cm$^{-1}$ (CONOH). $^1$H-NMR (80 MHz, $CDCl_3$): $\delta$ 7.32 (m, 5H, ArH), 5.77 (d, 1H, NH), 5.0 (ABq, 2H, $ArCH_2$), 4.81 (m, 1H, CH-*i*-Bu), 3.21 (s, 3H, $NCH_3$), and 0.92 ppm (d, 6H, $J$ = 4.5 Hz, $(CH_3)_2$).

**Preparation of Cbz-L-NHCH(CH$_3$)CONOHCH$_3$ (7A).** Using the same procedure as for hydroxamate **7L**, the ala derivative **7A** is prepared and purified by flash chromatography on silica gel ($CCl_4$–EtOAc, 90:10, 80:20, and 70:30) in 80% yield. Mp: 105–110 °C. IR ($CDCl_3$): $\nu$ 1699 (OCONH), 1648 cm$^{-1}$ (CONOH). $^1$H-NMR (270 MHz, $CDCl_3$): $\delta$ 9.0 (s, 1H, NOH), 7.32 (m, 5H, ArH), 5.72 (d, 1H, $J$ = 12.1, NH), 4.99 and 5.10 (ABq, 2H, $ArCH_2$), 4.85 (m, 1H, CHMe), 3.23 (s, 3H, $NCH_3$), and 1.34 ppm (d, 3H, $J$ = 6.8 Hz, s, 9H, $CCH_3$).

**Preparation of Boc-NHCH$_2$CONOHCH$_3$ (7G).** Following the same procedure as for **7L**, the hydroxamate **7G** is obtained in 95% yield after chromatographic purification on silica gel ($CHCl_3$ and then $CHCl_3$–MeOH, 96:4). Mp: 98–100 °C. IR ($CDCl_3$): $\nu$ 1654 cm$^{-1}$ (OCONH). NMR (270 MHz, $CDCl_3$): $\delta$ 5.52 (broad, 1H, NH), 4.07 (d, $J$ = 4.9 Hz, 2H, $NCH_2CO$), 3.27 (s, 3H, $NCH_3$), and 1.45 ppm ($C(CH_3)_3$).

**Preparation of Boc-L-NHCH(*s*-Bu)CONOHCH$_3$ (7I).** Using the same procedure as for **7L**, hydroxamate **7I** is prepared in 23% yield. Purification by chromatography on silica gel ($CHCl_3$ and then $CHCl_3$–MeOH, 99:1). Mp: 98–100 °C. IR ($CDCl_3$): $\nu$ 1704 (OCON), 1678, 1637 cm$^{-1}$ (CON). $^1$H-NMR (270 MHz, $CDCl_3$): $\delta$ 5.25 (m, 1H, BocNH), 4.60 (t, 1H, CH(*s*-Bu), 3.26 (s, 3H, $NCH_3$), and 1.42 ppm (s, 9H, $C(CH_3)_3$).

**Preparation of Cbz-L-NCH$_2$CH$_2$CH$_2$CHCONOHCH$_3$ (7P).** A solution containing 4.42 g (8.88 mmol) of active ester **6P** dissolved in 20 mL of dry $CH_2Cl_2$ is added to a solution containing 1.05 g (12.35 mmol) of *N*-methylhydroxylamine hydrochloride, 1.8 mL of $Et_3N$, and 50 mg of *N*-hydroxysuccinimide in 40 mL of dry $CH_2Cl_2$. The solution is stirred for 2 days at room temperature. The solvent is removed, and the crude mixture is chromatographed on silica gel ($CHCl_3$ and then $CHCl_3$–MeOH, 95:5) to give product **7P** in 43% yield as an oil. IR (neat): $\nu$ 1680 (OCON), 1645 cm$^{-1}$ (CONOH). $^1$H-NMR (80 MHz, $CDCl_3$): $\delta$ 7.33 (m, 5H, ArH), 5.11 (s, 2H, $ArCH_2$), 4.94 (m, 1H, CH), 3.56 (m, 2H, $NCH_2$), 3.23 (s, 3H, $NCH_3$), and 2.09 ppm (m, 4H, $CH_2CH_2$).

**Preparation of L-NH$_2$CH(*i*-Bu)CONOHCH$_3$ (5L).** A solution of 2.4 g (8.16 mmol) of protected hydroxamate **7L** in 70 mL ethanol is added to a suspension of 0.813 g of Pd/C (5%) in 30 mL of ethanol. The mixture is hydrogenated under atmospheric pressure for 45 min. The mixture is filtered and evaporated to dryness to provide **5L** as an oil in 97% yield. IR ($CDCl_3$): $\nu$ 1648 cm$^{-1}$ (CONOH). $^1$H-NMR (270 MHz, $CDCl_3$): $\delta$ 5.19 (broad, 3H, $NH_2$ and NOH), 4.08 (m, 1H, CH-*i*-Bu), 3.23 (s, 3H, $NCH_3$), and 0.95 ppm (several signals, 6H, $(CH_3)_2$).

**Preparation of L-NH$_2$CH(CH$_3$)CONOHCH$_3$ (5A).** Using the same procedure as for hydroxamate **5L**, the ala derivative **5A** is obtained in 95% yield as an oil. IR ($CDCl_3$): $\nu$ 1650 cm$^{-1}$ (CONOH). $^1$H-NMR (270 MHz, $CD_3OD$): $\delta$ 4.12 (m, 1H, CHMe), 3.22 (s, 3H, $NCH_3$), and 1.28 ppm (d, 3H, $J$ = 6.6 Hz, $CCH_3$).

**Preparation of CF$_3$COOHH$_2$NCH$_2$CONOHCH$_3$ (5G).** The hydroxamate salt **5G** is prepared by treating 485 mg (2.5 mmol) of the protected hydroxamate **7G** for 30 min at room temperature with a 2:1 mixture of methylene chloride and trifluoroacetic acid. The salt obtained after removal of excess trifluoracetic acid and solvent is used without further purification.

**Preparation of CF$_3$COOHH$_2$NCH(*s*-Bu)CONOHCH$_3$ (5I).** The salt **5I** is obtained according to the same procedure as **5G** and used without further purification.

**Preparation of L-NHCH$_2$CH$_2$CH$_2$CHCONOHCH$_3$ (5P).** A solution of 3.51 g (0.012 mol) of hydroxamate **7e** in 100 mL of ethanol is added to 0.55 g of Pd/C (10%) suspended in 20 mL of EtOH. The mixture is hydrogenated under atmospheric pressure for 30 min. After the usual workup, the crude is chromatographed on silica gel ($CHCl_3$–MeOH, 8:2) to afford the free amine **5P** in 77% yield as an oil. IR (neat): $\nu$ 1660 cm$^{-1}$ (CONOH). $^1$H-NMR (80 MHz, DMSO): $\delta$ 6.25 (broad, 2H, NH and OH), 4.47 (t, 1H, $J$ = 7.2 Hz, CH), 3.17 (s, 3H, $NCH_3$), 2.88 (m, 2H, $NCH_2$), and 1.87 ppm (m, 4H, $CH_2CH_2$).

**Preparation of EtC(CH$_2$OCH$_2$CONOHCH$_3$)$_3$ (1).** A solution containing 1 g (0.94 mmol) of trisphenolate **3** is dissolved in 20 mL of dry $CH_2Cl_2$ and added to a suspension containing 0.334 g (4 mmol) of *N*-methylhydroxylamine hydrochloride and 0.55 mL of triethylamine in dry $CH_2Cl_2$. The mixture is stirred during 3 days at room temperature,

then diluted with $CH_2Cl_2$, and washed with $H_2O$. The aqueous phase is subjected to liquid–liquid extraction with ethyl acetate. The organic phase (EtOAc layer) is evaporated to provide the product **1** in 20% yield after precipitation from MeOH/EtOEt as a white powder. Mp: 87–90 °C.

**Preparation of $EtC(CH_2OCH_2CH_2CONOHCH_3)_3$ (2).** A 1.08-g amount (0.985 mmol) of trisphenolate **4** is dissolved in 50 mL of dry $CH_2Cl_2$. To the solution is added a suspension containing 0.336 g (4 mmol) of *N*-methylhydroxylamine hydrochloride, 0.6 mL of triethylamine, and 50 mg of *N*-hydroxysuccinimide in methylene chloride. The mixture is stirred during 3 days at room temperature. The solvent is evaporated, and the crude mixture is chromatographed on silica gel ($CHCl_3$ and then $CHCl_3$–MeOH, 95:5) to provide trishydroxamate **2** in 73% yield as an oil.

**Preparation of $EtC(CH_2OCH_2CONHCH(i\text{-}Bu)CONOHCH_3)_3$ (1L).** A 0.987-g amount (0.937 mmol) of trisphenolate **3** is dissolved in 20 mL of dry methylene chloride. Then 0.6 g (3.75 mmol) of amine **5L** and 54 mg of *N*-hydroxysuccinimide are added to the solution, and the reaction mixture is stirred for 3 days at room temperature. The solvent is evaporated, and the crude mixture is chromatographed on silica gel ($CHCl_3$–MeOH, 98:2, and then $CHCl_3$–MeOH, 95:5) to give the desired product **1L** in 38% yield as a glassy solid. Mp: 68–72 °C.

**Preparation of $EtC(CH_2OCH_2CONHCH(CH_3)CONOHCH_3)_3$ (1A).** The same procedure as for compound **1L** is employed for synthesizing the trishydroxamate **1A**. The latter is purified by chromatography on silica gel ($CHCl_3$–MeOH, 95:5, 93:7, and then 90:10) and obtained in 21% yield as an oil.

**Preparation of $EtC(CH_2OCH_2CONHCH_2CONOHCH_3)_3$ (1G).** A 0.31-g amount (0.29 mmol) of active ester **3** and 33 mg of *N*-hydroxysuccinimide are dissolved in 6 mL of methylene chloride, and the mixture is treated with a solution of 1.2 mmol of hydroxamate salt **5G** in 6 mL of methylene chloride that had been neutralized by addition of triethylamine. The mixture is stirred for 2 days at room temperature, concentrated, and purified by two successive chromatographies on silica gel ($CH_2Cl_2$–MeOH and EtOAc–*i*-PrOH–AcOH, respectively) to give 60% of a colorless solid. Mp: 118–120 °C.

**Preparation of $EtC(CH_2OCH_2CH_2CONHCH(i\text{-}Bu)CONOHCH_3)_3$ (2L).** Using the same procedure as for compound **1L**, the trishydroxamate **2L** is prepared by using the trisphenolate **4** and by adding 200 mg of imidazole. Purification by chromatography on silica gel ($CHCl_3$ and then $CHCl_3$–MeOH, 95:5) gave the desired product **2L** in 35% yield as a glassy solid. Mp: 77–80 °C.

**Preparation of $EtC(CH_2OCH_2CH_2CONHCH(CH_3)CONOHCH_3)_3$ (2A).** A 1.3-g amount (1.2 mmol) of active ester **4** is dissolved in 60 mL of methylene chloride together with 250 mg of *N*-hydroxysuccinimide and 200 mg of imidazole, and the mixture is treated with a solution of 400 mg (3.7 mmol) of **5A** dissolved in 3 mL of dimethylformamide. The mixture is stirred for 1 day, concentrated in vacuo, and chromatographed on silica gel ($CHCl_3$ and $CHCl_3$–MeOH, 95:5) to provide the trishydroxamate **2A** in 35% yield as an oil.

**Preparation of $EtC(CH_2OCH_2CH_2CONHCH_2CONOHCH_3)_3$ (2G).** A 680-mg amount (0.6 mmol) of active ester **4** is dissolved in 10 mL of methylene chloride; 40 mg of *N*-hydroxysuccinimide and 40 mg of (dimethylamino)pyridine are added. To this mixture is then added a solution of salt **5G** (2.5 mmol) in 6 mL of methylene chloride and 10 drops of dimethylformamide that had been neutralized with triethylamine. The mixture is stirred for 2 days at room temperature, concentrated, and purified by chromatography on silica gel ($CHCl_3$ and then $CHCl_3$–MeOH, 95:5). Mp: 53–55 °C (highly hydroscopic).

**Preparation of $EtC(CH_2OCH_2CH_2CONHCH(s\text{-}Bu)CONOHCH_3)_3$ (2I).** A 350-mg amount (0.32 mmol) of active ester **4** is dissolved in 15 mL of methylene chloride together with 50 mg of *N*-hydroxysuccinimide and 15 mg of imidazole, and the mixture is treated with a solution of 1.28 mmol of salt **5I**, which had been dissolved in 5 mL of acetonitrile and neutralized with triethylamine. The mixture is stirred for 2 days at room temperature, concentrated, and chromatographed on silica gel ($CHCl_3$–MeOH, 95:5) to provide the trishydroxamate in 62% yield. Mp: 55–58 °C.

**Preparation of $EtC(CH_2OCH_2CH_2CONCH_2CH_2CH_2CHCONOHCH_3)_3$ (2P).** A 2.61-g amount (2.38 mmol) of trisphenolate **4** is dissolved in 30 mL of dry $CH_2Cl_2$ and 20 mL of DMF. Then 1.413 g (9.8 mmol) of **5P** dissolved in 15 mL of DMF, 500 mg of imidazole, and 150 mg of *N*-hydroxysuccinimide are added to the solution. The reaction mixture is stirred for 2 days. The solvent is evaporated, and the crude mixture is chromatographed on silica gel ($CHCl_3$–MeOH, 95:5 and then 90:10) to give the desired product **2P** in 14% yield. Mp: 34–38 °C.

**Acknowledgment.** The authors thank the U.S.-Israel Binational Science foundation for support of this work, Professor S. Lifson for enlightening discussions, and Mrs. Rahel Lazar for her skillful technical assistance. The collaboration of Professor R. Bauminger of the Hebrew University in the Mössbauer work is much appreciated. A.S. is the holder of the Siegfried and Irma Ullmann Professorial Chair.